Hellmann-Feynman theorem and correlation-fluctuation analysis for the Calogero-Sutherland model

2001 J. Phys. A: Math. Gen. 34 1485

(http://iopscience.iop.org/0305-4470/34/7/320)

INSTITUTE OF PHYSICS PUBLISHING JOURNAL OF PHYSICS A: MATHEMATICAL AND GENERAL

J. Phys. A: Math. Gen. **34** (2001) 1485–1506 www.iop.org/Journals/ja PII: S0305-4470(01)16871-X

Hellmann–Feynman theorem and correlation-fluctuation analysis for the Calogero–Sutherland model

Rudolf A Römer[1] **and Paul Ziesche**[2]

[1] Institut für Physik, Technische Universität, D-09107 Chemnitz, Germany
[2] Max-Planck-Institut für Physik komplexer Systeme, Nöthnitzer Straße 38, D-01187 Dresden, Germany

E-mail: r.roemer@physik.tu-chemnitz.de

Received 4 September 2000, in final form 19 December 2000

Abstract

Exploiting the results of the exact solution for the ground state of the one-dimensional spinless quantum gas of fermions and impenetrable bosons with the μ/x_{ij}^2 particle–particle interaction, the Hellmann–Feynman theorem yields mutually compensating divergences of both the kinetic and the interaction energy in the limiting case $\mu \to -\frac{1}{4}$. These divergences result from the peculiar behaviour of both the momentum distribution (for large momenta) and the pair density (for small inter-particle separation). The available analytical pair densities for $\mu = -\frac{1}{4}, 0$ and 2 allow one to analyse particle-number fluctuations. They are suppressed by repulsive interaction ($\mu > 0$), enhanced by attraction ($\mu < 0$), and may therefore measure the kind and strength of correlation. Other recently proposed purely quantum-kinematical measures of the correlation strength arise from the small-separation behaviour of the pair density or—for fermions—from the non-idempotency of the momentum distribution and its large-momenta behaviour. They are compared with each other and with reference-free, short-range correlation-measuring ratios of the kinetic and potential energies.

PACS numbers: 7110, 7110P, 0540, 7145

1. Introduction

In the ground state of electron systems, it has been shown that exchange (X) due to the Pauli 'repulsion' and correlation (C) due to the Coulomb repulsion suppress particle-number fluctuations and consequently reduce the energy [1–3]. This energy reduction provides most of the 'glue' that binds atoms together to form molecules and solids [4]. Particle-number fluctuations mean that the particle number in a domain (which may be a muffin-tin sphere, a Wigner–Seitz cell, a Bader basin [5], a Daudel loge [6], a bond region between atoms in a

molecule, etc) fluctuates due to zero-temperature quantum motion with a certain probability. Fulde [1] takes C_2H_2 as an example for such fluctuations. The number of valence electrons in a sphere containing a C atom fluctuates around its average value ≈ 3.9. Comparison of Hartree–Fock (HF) calculations for C_2H_2 with calculations which include correlation shows that configurations with large deviations from the average valence electron number (e.g. with zero and one or seven and eight electrons) are strongly suppressed due to correlation. A similar fluctuation–correlation analysis is performed in [2] for several dimers and in [3][3] for the uniform electron gas in one, two and three dimensions (1D, 2D, 3D). These calculations for the above-mentioned narrowing of the particle-number distribution need the pair density (PD) $n(\vec{r}_1, \vec{r}_2)$ and this narrowing is used to derive from the PD a quantum-kinematical measure of the correlation strength [1]. Correlation and its strength is furthermore characterized by the small-separation (or on-top) behaviour of the PD. The spherically averaged on-top curvature of the spin-parallel PD may serve as a local correlation measure [7] and from the topological analysis of the intracule PD a short-range correlation strength is defined [8]. In addition to these PD-based quantities the concept of a correlation 'entropy' has been developed for Fermi systems [9–12][4] (in [11] the term Jaynes entropy is used). It is based on the correlation induced non-idempotency of the correlated one-particle density matrix (1PDM) $\gamma(\vec{r}; \vec{r}')$. All these correlation measures intend to make the qualitative terms 'weak and strong correlation' quantitatively precise [13]. Note that strong correlation means extreme narrowing of the particle-number distribution, which is usually described as electron localization.

In the present paper, we apply the above-mentioned fluctuation–correlation analysis to the exactly solvable Calogero–Sutherland (CS) model [14]. The CS model is a model of long-range-interacting spinless particles in 1D and has been solved exactly by means of the (asymptotic) Bethe-ansatz technique [14, 15]. The solution is valid for both fermionic and bosonic particle symmetry. Here we will mostly concentrate on the Fermi systems. Furthermore, the model can be shown to be the universal quantum model underlying the dynamical interpretation of random matrix theory [16, 17]. This latter connection has been used to also compute several correlation functions exactly at three special values of the interaction strength, among which are the 1PDM and the PD [14]. Thus although the information is restricted to the 1D case, the model nevertheless is ideally suited for testing the fluctuation–correlation measures discussed above.

Correlated 1PDM and correlated PD need correlated many-body wavefunctions (beyond the HF caricature), which in quantum chemistry [18, 19] are traditionally obtained from configuration-interaction, coupled-cluster, Møller–Plesset, quantum Monte Carlo calculations or recently from the contracted-Schrödinger-equation method [20] or the incremental method [21]. All of these procedures involve certain approximations or have restricted applicability. So the existence of non-trivial *exactly solvable models* which can provide 1PDM and PD is of much interest for the mentioned fluctuation and correlation analysis.

We shall only consider the ground state properties of the CS model [14]. The interaction is pairwise inversely proportional to the square of the distance $x_{ij} = |x_i - x_j|$ of two particles with interaction strength μ, i.e. μ/x_{ij}^2. The interaction strength $\mu \geqslant -\frac{1}{4}$ is occasionally parametrized as $\mu = \lambda(\lambda - 1)$ with a parameter $\lambda = \frac{1}{2} + \sqrt{\frac{1}{4} + \mu} \geqslant \frac{1}{2}$. We shall mostly use the parametrization $\nu = \sqrt{\frac{1}{4} + \mu}$, such that $\mu = \nu^2 - \frac{1}{4}$ and $\lambda = \frac{1}{2} + \nu$.

[3] Here it is shown how particle fluctuation is reduced by exchange in the ideal Fermi gas and further reduced by Coulomb correlation in the interacting electron gas of one, two or three dimensions.

[4] In [9] the meaning of $\mathrm{Tr}(\gamma - \gamma^2)$ is sought, which is in our notation $Nc(2)$.

In the thermodynamic limit we assume constant density $\rho(x) = n$, so the CS ground state has only two parameters, ν and n. The $1/x_{ij}^2$ interaction has the peculiarity of not possessing a natural length. Therefore, it is a model showing critical behaviour, which can be discussed in terms of universality classes and their conformal anomalies [22–25]. This beauty of the $1/x_{ij}^2$ interaction also shows up in the analytical Bethe ansatz solutions [14, 26–30] and the explicit knowledge of the correlated many-body wavefunctions [14, 31]. From the Bethe ansatz technique the complete energy spectrum and in particular the ground state energy per particle as a function of the interaction strength parameter ν is available [14]. We show that its kinetic and interaction 'components' can be deduced with the help of the Hellmann–Feynman theorem [32][5]. Surprisingly, when the interaction strength parameter ν approaches its limiting value 0, both the kinetic and the interaction energy diverge in such a way that they compensate each other, leaving the total energy finite. As we outline in the following, these divergences result from the peculiar behaviour of the 1PDM and the PD for $\nu \to 0$ and are related to the 'fall-into-the-origin' already mentioned in [33].

For $\nu = 0, \frac{1}{2}$, and $\frac{3}{2}$—corresponding to $\mu = -\frac{1}{4}, 0$ and 2 or $\lambda = \frac{1}{2}$, 1, and 2—it has been shown [14] that the square of the ground state wavefunction is intimately related to the eigenvalue distribution of random matrices of the orthogonal ensemble, the unitary ensemble and the symplectic ensemble, respectively. Using this connection, Sutherland had shown how to construct the 1PDM and the PD using integral relations of random matrix theory. The resulting formulae reduce the problem, say for the 1PDM, from the evaluation of a high-dimensional integral to the computation of a determinant of a matrix [15]. From the 1PDM $\gamma(x-x')$, the momentum distributions n_κ for the three special values of ν follow via the Fourier transform. Due to correlation the latter quantities are non-idempotent. They determine the mentioned correlation entropy per particle $s = -\sum_\kappa n_\kappa \ln n_\kappa / \sum_\kappa n_\kappa$. Knowledge of the PD $n(x_{12})$ allows [14, 15, 34, 44] us to calculate the fluctuation ΔN_X of the particle number around its mean value $N_X = nX$ in any piece (domain) X of the x-axis. Comparing this variance of the particle-number distribution $P_X(N)$ for the cases of 'no correlation' ($\nu = \frac{1}{2}$ or HF approximation) and 'correlation' shows the above-mentioned narrowing for repulsion ($\nu > \frac{1}{2}$) in a smaller ΔN_X. In contrast, for attraction ($\nu < \frac{1}{2}$) a broadening with a larger ΔN_X appears.

In section 2, we introduce the CS model, define the kinematical quantities used throughout the text, and present the Hellmann–Feynman theorem. Section 3 is devoted to the thermodynamic limit. In section 4, after presenting the HF approximation, we discuss first qualitatively and then analytically the influences of the CS interaction on 1PDM and PD. In particular, we show that the above-mentioned divergences in kinetic and potential energies are caused by a peculiar behaviour of the PD $n(x_{ij})$ for *small inter-particle separations* $x_{ij} \ll k_F^{-1}$ and of the momentum distribution n_κ for *large momenta* $k \gg k_F$ or $\kappa \equiv k/k_F \gg 1$. In section 5 we then apply the mentioned fluctuation–correlation measures to the CS model. Section 6 is devoted to details of the numerics and in section 7 we discuss extensions of our approach to impenetrable bosons and lattice gases. We conclude in section 8 with a discussion of our results.

[5] What is usually referred to as the Hellmann–Feynman theorem was first formulated by Güttinger [48], see his equation (11). This result is implicitly contained in equation (28) of Born and Fock [49]. Whereas in these papers any parameter is considered, Hellmann and later Feynman explicitly referred to the special case of nuclear coordinates within the Born–Oppenheimer approximation, leading to the Hellmann–Feynman forces upon nuclei. Within perturbation theory the theorem was already given by Schrödinger [50]. Thus the theorem is due to Schrödinger, Born, Fock, Güttinger, Hellmann and Feynman.

2. The system and its ground state

2.1. Hamiltonian, energies and quantum kinematical quantities

The Hamiltonian of the CS model is $\hat{H} = \hat{T} + \hat{V}$ with

$$\hat{T} = \sum_i^N \tfrac{1}{2} p_i^2 \qquad \hat{V} = \sum_i^N v_{\text{ext}}(x_i) + \sum_{i<j}^N \frac{\nu^2 - \frac{1}{4}}{x_{ij}^2} \tag{2.1}$$

with $p_i^2 = -\partial^2/\partial x_i^2$, and N equal to the number of particles. We assume the system to be confined to the length L by an external potential $v_{\text{ext}}(x)$, for example, a box or harmonic oscillator potential. In the following we alternatively assume periodic boundary conditions with $v_{\text{ext}}(x) = 0$ and a density in the k space described by $L\Delta k/(2\pi) = 1$ [14][6]. The average particle density is $n = N/L$. Furthermore, it follows from dimensional arguments that all energies for the Hamiltonian (2.1) are proportional to n^2 in agreement with the virial theorem and all lengths are measured in units of $1/n$ (thus $k_{\text{F}} \sim n$) [14].

We denote the ground state energy and its kinetic and potential 'components' by $E_N = \langle \hat{H} \rangle$, $T_N = \langle \hat{T} \rangle$ and $V_N = \langle \hat{V} \rangle$, respectively. Then the corresponding energies per particle are $e_N = E_N/N$, $t_N = T_N/N$, $v_N = V_N/N$ with $e_N = t_N + v_N$. From the antisymmetric (or symmetric) ground state wavefunction follow by contractions [14, 15] the 1PDM $\gamma_N(x; x')$ and the PD $n_N(x_1, x_2)$ normalized as $\int \mathrm{d}x \gamma_N(x; x) = N$ and $\int \mathrm{d}x_1 \int \mathrm{d}x_2\, n_N(x_1, x_2) = N(N-1)$, respectively. The PD describes the XC hole, vanishing for zero separation and approaching the Hartree product $\rho_N(x_1)\rho_N(x_2)$ for large separations. The cumulant PD $w_N(x_1, x_2) \equiv \rho_N(x_1)\rho_N(x_2) - n_N(x_1, x_2)$ is size-extensively normalized via

$$\int \mathrm{d}x_1 \int \mathrm{d}x_2\, w_N(x_1, x_2) = N. \tag{2.2}$$

Furthermore, with the abbreviation $y = k_{\text{F}} x$, $k_{\text{F}} = \pi n$ [14], and with the *dimensionless functions* $f_N(y_1; y_2)$ hermitian, $g_N(y_1, y_2)$ non-negative, and $h_N(y_1, y_2) \equiv f_N(y_1; y_1) f_N(y_2; y_2) - g_N(y_1, y_2)$, we can write for the 1PDM $\gamma_N(x_1; x_2) = n f_N(y_1; y_2)$, for the PD $n_N(x_1, x_2) = n^2 g_N(y_1, y_2)$, and for the cumulant PD we have $w_N(x_1, x_2) = n^2 h_N(y_1, y_2)$. The dimensionless cumulant PD is normalized as

$$\frac{1}{N} \int \frac{\mathrm{d}y_1}{\pi} \frac{\mathrm{d}y_2}{\pi}\, h_N(y_1, y_2) = 1 \tag{2.3}$$

which follows from equation (2.2). With these dimensionless 1PDM and PD and with the Fermi energy $\epsilon_{\text{F}} = k_{\text{F}}^2/2$ the energies t_N and v_N are given by

$$t_N = \frac{1}{N} \int \frac{\mathrm{d}y_1}{\pi} \left[-\frac{\partial^2}{\partial y_1^2} f_N(y_1; y_2) \right]_{y_2 = y_1} \epsilon_{\text{F}} \tag{2.4a}$$

and

$$v_N = \frac{1}{N} \int \frac{\mathrm{d}y_1}{\pi} \frac{\mathrm{d}y_2}{\pi} g_N(y_1, y_2) \frac{\nu^2 - \frac{1}{4}}{y_{12}^2} \epsilon_{\text{F}}. \tag{2.4b}$$

Therefore, t_N/ϵ_{F}, v_N/ϵ_{F} and e_N/ϵ_{F} are functions of ν and N. The latter dependence disappears for the thermodynamic limit as shown in section 3.

[6] We emphasize that the replacement $\mu/x_{ij}^2 \to \mu/[L \sin(\pi x_{ij}/L)/\pi]^2$ is used for periodic systems as discussed in [14, 15].

2.2. The Hellmann–Feynman theorem

If e_N is known as a function of $\mu = \nu^2 - \frac{1}{4}$, then t_N and v_N can be obtained from the Hellmann–Feynman theorem [32] without knowing the quantum-kinematical quantities $f_N(y_1; y_2)$ and $g_N(y_1, y_2)$. This theorem states that

$$\frac{\partial E_N}{\partial \mu} = \left\langle \frac{\partial \hat{H}}{\partial \mu} \right\rangle \tag{2.5}$$

which for (2.1) gives

$$v_N = \mu \frac{\partial e_N}{\partial \mu} \qquad t_N = \left(1 - \mu \frac{\partial}{\partial \mu}\right) e_N \tag{2.6}$$

and also

$$\frac{\partial}{\partial \mu} t_N = -\mu \frac{\partial}{\partial \mu} \left(\frac{1}{\mu} v_N\right). \tag{2.7}$$

Thus—with equation (2.4) in mind—the Hellmann–Feynman relation (2.5) for the $1/x_{ij}^2$ model establishes an integral relation between the dimensionless 1PDM f_N on the left-hand side and the dimensionless PD g_N on the right-hand side of equation (2.7).

3. Thermodynamic limit

We wish to study the thermodynamic limit with $N \to \infty$ and $L \to \infty$ such that $n = N/L =$ constant. The resulting extended system has only two parameters, the interaction strength parameter ν and the Fermi wavenumber k_F. So t/ϵ_F, v/ϵ_F and e/ϵ_F become functions of ν only. Furthermore, the thermodynamic limit makes the 1PDM and the PD to depend only on $k_F x_{12} \equiv k_F |x_1 - x_2| = |y_1 - y_2| \equiv y_{12}$. The dimensionless functions f_N, g_N and h_N then take the forms $f(y_{12})$, $g(y_{12})$ and $h(y_{12}) = 1 - g(y_{12})$, respectively, with $f(0) = 1$ and $g(0) = 0$ or equivalently $h(0) = 1$. These functions have ν as the only parameter.

The eigenfunctions (or natural orbitals) of the 1PDM $\gamma(x_{12}) = nf(y_{12})$ become simply plane waves $\varphi_k^0(x) = \mathrm{e}^{\mathrm{i}kx}/\sqrt{L}$, such that

$$\gamma(x_{12}) = n \int_0^\infty \mathrm{d}\kappa \, n_\kappa \cos \kappa y_{12} \equiv nf(y_{12}) \tag{3.1}$$

where n_κ is the momentum distribution and $\kappa = k/k_F$.

For $\nu = \frac{1}{2}$ (ideal spinless 1D Fermi gas) the Pauli principle leads in the reciprocal space to the Fermi ice block $n_\kappa^0 = \theta(1 - |\kappa|)$ and in the direct space to the ideal X hole $g^0(y) = 1 - [f^0(y)]^2$ with the dimensionless 1PDM $f^0(y) = (\sin y)/y$ following from equation (3.1). The energy per particle is $e_0 = \epsilon_F/3 = k_F^2/6$.

In general, with $\gamma(0) = n$, the momentum distribution n_κ is normalized as $\sum_\kappa n_\kappa = N$ or

$$\int_0^\infty \mathrm{d}\kappa \, n_\kappa = 1. \tag{3.2}$$

The kinetic energy per particle is according to equation (2.4*a*)

$$t = 6 \int_0^\infty \mathrm{d}\kappa \, n_\kappa \frac{\kappa^2}{2} e_0 \tag{3.3}$$

where n_κ is a function of $|\kappa|$ and ν, so t/e_0 is a function of ν only with $t = e_0$ for $\nu = \frac{1}{2}$ as shown in figure 1.

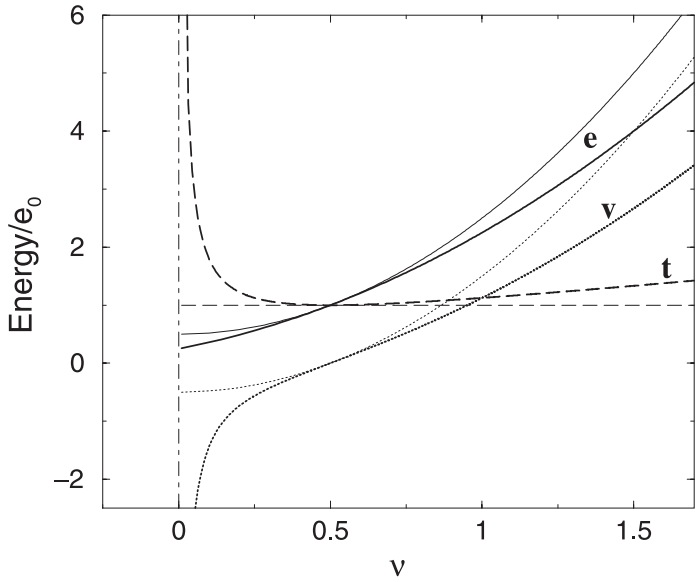

Figure 1. Bulk energy e (full), kinetic energy t (broken), and potential energy v (dotted) plotted as functions of interaction strength parameter ν. Thin curves denote the results of the Hartree–Fock approximation, thick curves are exact. The thin chain curve indicates the 'fall-into-the-origin' at $\nu = 0$.

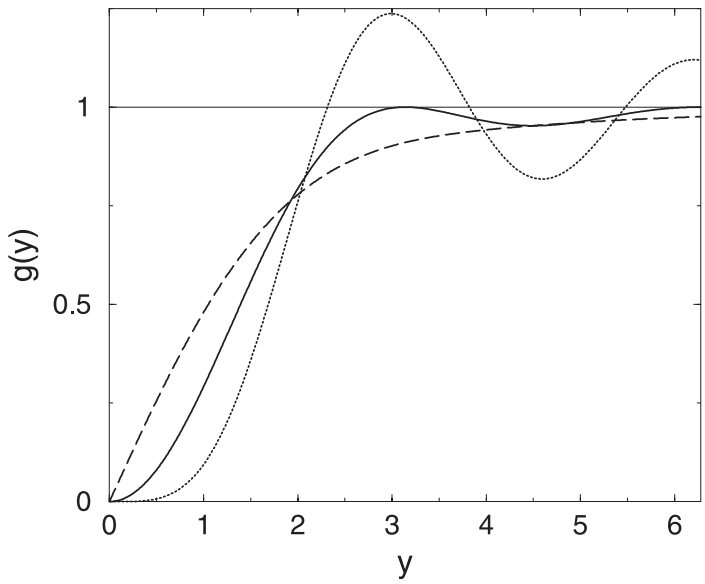

Figure 2. Dimensionless PD $g(y) = n(x_{12})/n^2$ as a function of the dimensionless inter-particle separation $y = k_F x_{12}$ for $\nu = 0$ (broken), $\frac{1}{2}$ (full) and $\frac{3}{2}$ (dotted). The thin line is a guide to the eye only.

The corresponding expressions for the PD $g(y)$ are according to equation (2.3)

$$2\int_0^\infty \frac{\mathrm{d}y}{\pi}\, h(y) = 1 \qquad h(y) = 1 - g(y) \tag{3.4}$$

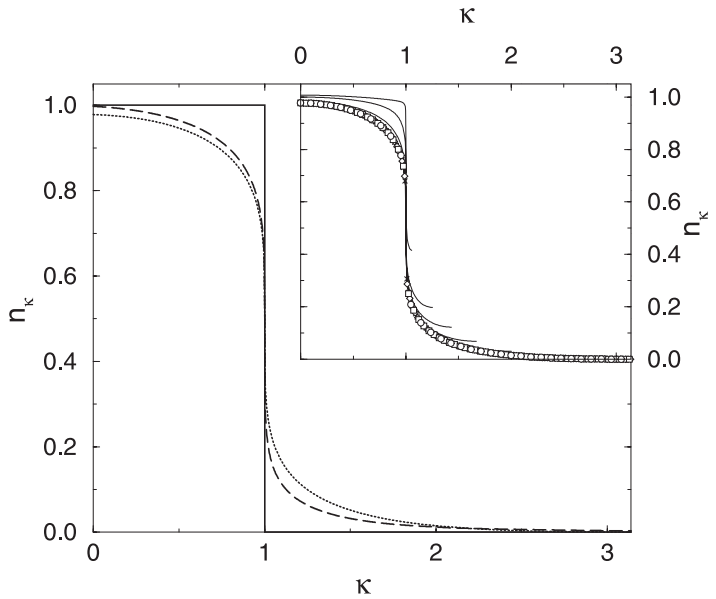

Figure 3. Fermionic momentum distributions n_κ versus $\kappa = k/k_F$ with $\nu = 0$ (broken), $\frac{1}{2}$ (full) and $\frac{3}{2}$ (dotted). Inset, n_κ for $\nu = \frac{3}{2}$ and $L = 401$ computed with $N = 21, 41, 81, 121, 161, 201, 241, 281, 321, 361$ and 401. The data for $N = 21(\circ), 41(\square), 81(\diamond)$ and $121(\times)$ do not show any density dependence, whereas the larger density data (curves) do.

and for the interaction energy per particle according to equation (2.4*b*)

$$v = 6\int_0^\infty \frac{\mathrm{d}y}{\pi}\, g(y)\frac{\nu^2 - \frac{1}{4}}{y^2}e_0 \tag{3.5}$$

where $g(y)$ is a function of y and ν, so v/e_0 is a function of ν only (see figure 1). With t and v follows the integral relation

$$\int_0^\infty \mathrm{d}\kappa\, \frac{\kappa^2}{2}\frac{\partial n_\kappa}{\partial \mu} = -\int_0^\infty \frac{\mathrm{d}y}{\pi}\frac{\mu}{y^2}\frac{\partial g(y)}{\partial \mu} \qquad \mu = \nu^2 - \tfrac{1}{4} \tag{3.6}$$

as a consequence of the Hellmann–Feynman theorem expressed in equation (2.7). Correlation via $\nu \neq \frac{1}{2}$ deforms the X hole and the Fermi ice block as shown in figures 2 and 3 in such a way that equation (3.6) is maintained.

4. Hartree–Fock approximation and correlation beyond it

4.1. Hartree–Fock approximation

The simplest approximation for the quantities n_κ, $g(y)$, t and v is obtained from the HF approach. The momentum distribution in equation (3.3) and the PD in equation (3.5) are to be replaced by their 'ideal' expressions n_κ^0 and $g^0(y)$, respectively. Consequently, we find $t_{HF} = e_0$ and $v_{HF} = 2\mu e_0$ and thus $e_{HF} = (1 + 2\mu)\, e_0$, as shown in figure 1. Here the identity (A.5) has been used. The total HF energy e_{HF} also obeys the Hellmann–Feynman theorem (2.5) and the virial theorem.

Table 1. On-top exponent and coefficients of the PD according to equation (4.1).

ν	0	$\frac{1}{2}$	$\frac{3}{2}$
α	1	2	4
A	$\frac{\pi}{6}$	$\frac{1}{3}$	$\frac{16}{135}$
a_1	0	0	0
a_2	$-\frac{1}{10}$	$-\frac{2}{15}$	$-\frac{8}{35}$
a_3	$\frac{2}{45\pi}$	0	0
a_4	$\frac{1}{280}$	$\frac{1}{105}$	$\frac{32}{1225}$
a_5	$-\frac{4}{1575\pi}$	0	0
a_6	$-\frac{1}{15\,120}$	$-\frac{2}{4725}$	$-\frac{2176}{1091\,475}$
a_7	$\frac{4}{55\,125\pi}$	0	0
a_8	$\frac{1}{1330\,560}$	$\frac{2}{155\,925}$	$\frac{125\,696}{1092\,566\,475}$

4.2. Qualitative discussion of correlation

Due to correlation the true ground state energy per particle, e, is below the HF energy e_{HF} and the true ground state wavefunction $\Phi(\cdots)$ is no longer a single Slater determinant. Note that the definition of the term 'correlation' needs a reasonable reference state, which is $\Phi_{\mathrm{HF}}(\cdots)$ in our case. So, correlation causes a negative correlation energy $e_{\mathrm{corr}} = e - e_{\mathrm{HF}} < 0$, namely through redistributions of $g^0(y)$ and n^0_κ which are shown in figures 2 and 3 and described in the following.

As we show in figure 2, correlation modifies the X hole of the unperturbed PD. In particular, the correlation induced changes for small y are of interest, because the interaction $1/y^2$ is there largest. The on-top behaviour of the uncorrelated X hole ($\nu = \frac{1}{2}$ or HF) is described by $g^0(y) = y^2/3 + \cdots$. In its correlated counterpart with a ν-dependent exponent and ν-dependent coefficients (see appendix B)

$$\begin{aligned} g(y) &= A y^\alpha \left(1 + a_1 y + a_2 y^2 + \cdots\right) \\ \alpha &= 1 + 2\nu \end{aligned} \tag{4.1}$$

correlation for $\nu \neq \frac{1}{2}$ shows up in $\alpha \neq 2$ and $A \neq \frac{1}{3}$. More precisely, repulsive particle interaction ($\nu > \frac{1}{2}$) supports the Pauli 'repulsion', so the X hole is broadened (through increasing α and decreasing A), but attractive particle interaction ($\nu < \frac{1}{2}$) fights against (or competes with) the Pauli 'repulsion', so the X hole is narrowed (through decreasing α and increasing A) as shown in figure 2 and table 1. This X hole narrowing (for $\nu < \frac{1}{2}$) or broadening (for $\nu > \frac{1}{2}$) makes

$$6 \int_0^\infty \frac{\mathrm{d}y}{\pi} \frac{g(y)}{y^2} = 1 + \frac{1}{2\nu} \gtrless 2 \qquad \text{for} \quad \nu \lessgtr \tfrac{1}{2}. \tag{4.2}$$

The equation follows from equation (4.8) below. Thus $v < v_{\mathrm{HF}} = 2\mu e_0$ for $\nu \neq \frac{1}{2}$ as shown in figure 1.

As shown in figure 3, correlation thaws the Fermi ice block $\theta(1 - |\kappa|)$. Mathematically, the momentum distribution n_κ becomes non-idempotent, physically this means that correlation excites particles for $\kappa > 1$ and holes for $\kappa < 1$. This increases the kinetic energy independent of whether the interaction is attractive ($\nu < \frac{1}{2}$) or repulsive ($\nu > \frac{1}{2}$): $t > t_{\mathrm{HF}}$ as can be seen in figure 1. We note that n_κ has no discontinuity at $|\kappa| = 1$. Its value is $\frac{1}{2}$ and

near $\kappa = 1$ it follows a power law as is typical for all Luttinger liquids with their $z_F = 0$ [35, 36].

We model the melting of the Fermi ice block analytically with the continuous function

$$n_\kappa = \tfrac{1}{2} + B(1-\kappa)^\beta \left[1 + b_1^-(1-\kappa)^\beta + b_2^-(1-\kappa)^{2\beta} + \cdots\right] \qquad \text{for} \quad 0 \leqslant \kappa \leqslant 1 \qquad (4.3a)$$

$$n_\kappa = \tfrac{1}{2} - B(\kappa-1)^\beta \left[1 + b_1^+(\kappa-1)^\beta + b_2^+(\kappa-1)^{2\beta} + \cdots\right] \qquad \text{for} \quad 1 \leqslant \kappa \leqslant 2 \qquad (4.3b)$$

$$n_\kappa = \frac{C}{\kappa^\gamma}\left(1 + \frac{c_2}{\kappa^2} + \frac{c_4}{\kappa^4} + \cdots\right) \qquad \text{for} \quad 2 \leqslant \kappa \leqslant \infty \qquad (4.3c)$$

with [15, 37]

$$\beta = \frac{1}{4}\frac{(1-2\nu)^2}{1+2\nu} \qquad (4.4)$$

and $\gamma = 3 + 2\nu$ (appendix B). The exponents β, γ and the coefficients B, C and $b_i^\pm$, c_i depend on ν. The condition $0 < \beta < 1$ ensures an infinite slope of n_κ at $\kappa = 1$. This n_κ has to obey the normalization (3.2) and the condition

$$3\int_0^\infty \mathrm{d}\kappa\, n_\kappa \kappa^2 = \frac{\left(\frac{1}{2}+\nu\right)^2}{2\nu} \geqslant 1 \qquad (4.5)$$

which follows from equation (4.7) below. For $\nu = \frac{1}{2}$ (or HF) it is $\beta = 0$, $B(1 + \sum_i b_i^\pm) = \frac{1}{2}$ and $C = 0$. The correlation-induced melting for $\nu \neq \frac{1}{2}$ shows up in $\beta > 0$, $B(1 + \sum_i b_i^\pm) < \frac{1}{2}$ and $C > 0$.

4.3. Results of the exact solution

With the help of the Bethe ansatz technique one obtains $e = \lambda^2 e_0$ [14, 15]. e as a function of the interaction strength parameter λ shows no special behaviour for $\lambda \underset{\to}{>} \frac{1}{2}$, but as a function of the interaction strength $\mu = \lambda(\lambda - 1)$,

$$e = \left(\tfrac{1}{2} + \nu\right)^2 e_0 \qquad \nu = \sqrt{\tfrac{1}{4} + \mu} \qquad (4.6)$$

the non-analytical behaviour for $\mu \to -\frac{1}{4}$ is obvious.

Equation (4.6) yields with the Hellmann–Feynman theorem (2.6) the kinetic energy per particle,

$$t = \frac{\left(\frac{1}{2}+\nu\right)^2}{2\nu} e_0. \qquad (4.7)$$

With equation (2.6) equation (4.6) also yields the interaction energy per particle

$$v = \mu\left(1 + \frac{1}{2\nu}\right) e_0. \qquad (4.8)$$

From figure 1 we see that both t and v diverge for $\nu \to 0$, while e remains finite.

Equations (4.7) and (4.8) lead to

$$\int_0^\infty \mathrm{d}\kappa\, n_\kappa \kappa^2 = 6\nu\left[\int_0^\infty \frac{\mathrm{d}y}{\pi}\frac{g(y)}{y^2}\right]^2 \qquad (4.9)$$

as another integral relation between the momentum distribution n_κ and the dimensionless PD $g(y)$ in addition to equation (3.6). These distribution functions have to change with ν in such a

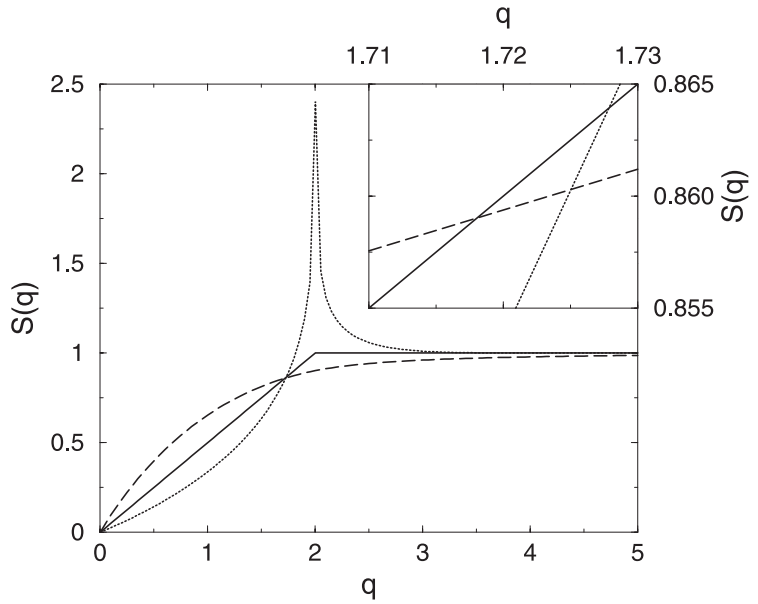

Figure 4. Static structure factor $S(q) = 1 - \tilde{h}(q)/\pi$ for $\nu = 0$ (broken), $\frac{1}{2}$ (full) and $\frac{3}{2}$ (dotted). Inset, the three curves do not coincide at a single point close to $q \approx 1.72$.

way that these relations (3.6) and (4.9) are obeyed together with the normalization conditions (3.2) and (3.4).

The PD $n(x_{12}) = n^2 g(y)$ with $y = k_F x_{12}$ is known analytically for the values $\nu = 0$, $\frac{1}{2}$, and $\frac{3}{2}$ [14, 15]. For $\nu = 0$ it is (with the notation of appendix A)

$$g(y) = 1 - \left(\frac{\sin y}{y}\right)^2 + \mathrm{Si}(y)\frac{\mathrm{d}}{\mathrm{d}y}\frac{\sin y}{y} - \frac{\pi}{2}\frac{\mathrm{d}}{\mathrm{d}y}\frac{\sin y}{y} \tag{4.10}$$

for $\nu = \frac{1}{2}$ (ideal Fermi gas) it is

$$g(y) = 1 - \left(\frac{\sin y}{y}\right)^2 \tag{4.11}$$

and for $\nu = \frac{3}{2}$ it is

$$g(y) = 1 - \left(\frac{\sin 2y}{2y}\right)^2 + \mathrm{Si}(2y)\frac{\mathrm{d}}{\mathrm{d}(2y)}\frac{\sin 2y}{2y}. \tag{4.12}$$

The corresponding dimensionless cumulant PDs $h(y) = 1 - g(y)$ are given in table 2 together with their Fourier transforms

$$\tilde{h}(q) = 2\int_0^\infty \mathrm{d}y \cos(qy)\, h(y). \tag{4.13}$$

They have via $S(q) = 1 - \tilde{h}(q)/\pi$ a simple relation to the static structure factor (or van Hove correlation function) $S(q) = \langle \hat{\rho}_q \hat{\rho}_q^\dagger \rangle / N$, which describes the correlation of density–density fluctuations. $\hat{\rho}_q = \sum_i \exp(-\mathrm{i}qx_i)$ is the Fourier transform of the density operator $\hat{\rho}(x) = \sum_i \delta(x - x_i)$. The three PDs $g(y)$ are shown in figure 2 and the three structure factors $S(q)$ in figure 4.

Table 2. Dimensionless cumulant PD $h(y)$ and the structure factor $S(q)$ used for the computation of ΔN_X and $\Sigma_1(\nu)$ as in equations (5.2) and (5.4).

ν	$h(y)$	$S(q) = 1 - \tilde{h}(q)/\pi$
0	$\left(\frac{\sin y}{y}\right)^2 - \left[\mathrm{Si}(y) - \frac{\pi}{2}\right]\frac{\mathrm{d}}{\mathrm{d}y}\frac{\sin y}{y}$	$\left[q - \frac{q}{2}\ln(1+q)\right]\theta(2-q) + \left[2 - \frac{q}{2}\ln\frac{q+1}{q-1}\right]\theta(q-2)$
$\frac{1}{2}$	$\left(\frac{\sin y}{y}\right)^2$	$\frac{q}{2}\theta(2-q) + \theta(q-2)$
$\frac{3}{2}$	$\left(\frac{\sin 2y}{2y}\right)^2 - \mathrm{Si}(2y)\frac{\mathrm{d}}{\mathrm{d}2y}\frac{\sin 2y}{2y}$	$\left[\frac{q}{4} - \frac{q}{8}\ln\lvert 1 - \frac{q}{2}\rvert\right]\theta(4-q) + \theta(q-4)$

For $\nu = \frac{1}{2}$ the weak oscillations of $g(y)$ and the (first-order) kink of $S(q)$ arise from the Fermi momentum distribution n_κ with its sharp discontinuity $z_\mathrm{F} = 1$ at $\kappa = 1$. With increasing repulsion the oscillations of $g(y)$ are enhanced, which is displayed in the reciprocal space by the peak of $S(q)$ at $q = 2$ (and a third-order kink at $q = 4$). This peak is customary in 1D quantum liquids (see, e.g., the spin-correlation functions of [38]). The first maximum of $g(y)$ runs through a certain trajectory from $(\pi, 1)$ to (2.99, 1.24). Whereas repulsion enhances the Friedel oscillations of $g(y)$ and the kink structure of $S(q)$, they diminish with increasing attraction: for $\nu = 0$ both $g(y)$ and $S(q)$ approach the value 1 smoothly (non-oscillatory) from below. The discontinuity for $\nu = 0$ of the second derivative of $S(q)$ at $q = 2$ replaces the kink seen for other values of ν. For the on-top behaviour of $g(y)$ in terms of $g(0)$, $g'(0)$, $g''(0)$ the following holds: it is $g(0) = 0$, according to the Pauli principle, $g'(0) = \pi/6$ for $\nu = 0$, but 0 for $\nu > 0$, and it is $g''(0) = 0$ for $\nu = 0$, infinite for $0 < \nu < \frac{1}{2}$, but $\frac{2}{3}$ for $\nu = \frac{1}{2}$, and 0 for $\nu > \frac{1}{2}$. We note that $S(q)$ and $g(y)$ can be also computed for other values of ν in addition to the three special values used here [34, 44].

With the identities (A.2)–(A.4) the normalization condition (3.4) is fulfilled. From equations (4.10)–(4.12) the on-top coefficients of equation (4.1) follow; they are shown in table 1. Note that the last two terms of equation (4.10) do not contribute to the normalization because of equation (A.3) and that the last term causes the odd on-top coefficients of table 1 and also the linear behaviour for small y. Its oscillations are exactly cancelled by the combined oscillations of the second and the third term. Simultaneously, these terms ensure the correct normalization.

The PD (4.11) for $\nu \to \frac{1}{2}$ plugged into equation (2.4*b*) yields with the identity (A.5) the same as results from equation (4.8), which follows from the total energy per particle, equation (4.6), and the Hellmann–Feynman theorem (2.6), namely $v = 2\mu e_0$. Similarly, the PD (4.12) for $\nu \to \frac{3}{2}$ plugged into equation (3.5) yields with the identities (A.5) and (A.6) the same as results from equation (4.8), namely $v = 4\mu e_0/3$.

For $\nu = 0$ a divergence appears, because from the PD (4.10) follows an on-top behaviour, which is linear in y as shown in figure 2 and table 1. This linear behaviour results from the last term of equation (4.10), which does not influence the normalization (3.4), but it makes the interaction energy $v \sim \int_0^\infty \mathrm{d}y\, g(y)/y^2$ diverge logarithmically in agreement with the divergence of $v \to -e_0/8\nu$ for $\nu \underset{\to}{>} 0$ as displayed in figure 1.

The divergence of the interaction energy is accompanied and compensated by the corresponding divergence of the kinetic energy $t \to e_0/8\nu$. This indicates a special asymptotic behaviour of the momentum distribution n_κ for $\nu \underset{\to}{>} 0$, namely equation (4.3*c*) with $\gamma \underset{\to}{>} 3$. For $\gamma > 3$ the integral $\int_0^\infty \mathrm{d}\kappa\, n_\kappa \kappa^2$ is convergent, but with $\gamma \underset{\to}{>} 3$ for $\nu \underset{\to}{>} 0$ it diverges logarithmically, whereas the normalization integral (3.2) remains convergent. The counterpart to this asymptotic behaviour of n_κ for $\kappa \to \infty$ is the on-top behaviour of the PD for $y \to 0$

Table 3. Coefficients as in equations (4.3*a*)–(4.3*c*) calculated from the numerically determined momentum distribution n_κ for $\nu = 0$ and $\frac{3}{2}$ (at $n = 1/2L_0$).

$\kappa \in [0,1]$		$\kappa \in [1,2]$		$\kappa \in [2,\infty]$	
$\nu = 0$					
B	0.863 355	B	0.863 355	C	0.017 788
b_1^-	−0.746 775	b_1^+	−0.750 439	c_2	5.972 791
b_2^-	0.731 357	b_2^+	0.747 380		
b_3^-	−0.420 828	b_3^+	−0.433 779		
		b_4^+	0.009 552		
$\nu = \frac{3}{2}$					
B	0.552 286	B	0.552 286	C	1.463 69
b_1^-	0.434 380	b_1^+	1.467 126	c_2	2.053 966
b_2^-	−0.570 516	b_2^+	−4.156 361		
		b_3^+	4.180 551		
		b_4^+	−1.606 130		

as shown in figure 2 and table 1 with a smooth transition of the coefficient A in equation (4.1) from $\pi/6$ via $\frac{1}{3}$, to $\frac{16}{135}$ for $\nu = 0$, $\frac{1}{2}$ and $\frac{3}{2}$, respectively. With quadratic interpolation of the coefficients shown in table 1 as functions of ν, one may continuously switch the on-top behaviour of the PD $g(y)$ between its forms at $\nu = 0$ and $\frac{3}{2}$. For the PD exponent $\alpha = 1 + 2\nu$ we refer to Appendix B, where also the momentum-distribution exponent is conjectured as $\gamma = 3 + 2\nu$.

These divergences of the kinetic and the interaction energies indicate that for attractive particle interaction μ/x_{ij}^2 with $\mu \to -\frac{1}{4}$ the system becomes unstable (no ground state with finite kinetic and potential energies). We note that it was shown in [33] that the singular particle interaction $-|\mu|/|\vec{r}_{12}|^2$ already makes two particles fall together ('fall-into-the-origin') for $|\mu| > \frac{1}{4}$ (ground state with $E \to -\infty$) and for $|\mu| < \frac{1}{4}$ there are only scattering states with $E \geqslant 0$ (no bound states with $E < 0$) [14].

For $\nu = 0$ the exact solution of the CS model yields the momentum-distribution data. In section 6 we will give the details of the necessary numerical calculation. The coefficients of equation (4.3*a*) are fitted to the n_κ values for $\kappa = 0 \ldots 1$ and the coefficients of equation (4.3*b*) are fitted to the n_κ values for $\kappa = 1 \ldots 2$. The coefficients are chosen to make also n_κ at $\kappa = 2$ continuous and smooth. Finally, b_3^+ is fine tuned to make the normalization equal to 1 according to (3.2). The results are shown in figure 3 and the values of the coefficients are given in table 3. The case $\nu = \frac{3}{2}$ is similarly treated only with the difference that also the kinetic energy $t = \frac{4}{3}e_0$ can be used for the fine tuning in addition to the normalization condition (3.2). The results are also shown in table 3. Here b_3^+ and b_4^+ have been used for fine tuning (which yields the normalization 0.997 and $t = 1.34e_0$, instead of 1 and $4e_0/3$).

5. Fluctuation–correlation analysis

5.1. Quantities following from the pair density

Particle-number fluctuations. Following Fulde [1] one may ask to what extent correlation influences particle-number fluctuations ΔN_X in a domain X, i.e. a certain interval of the x-axis, where on average there are $N_X = nX$ particles. These fluctuations are measured quantitatively

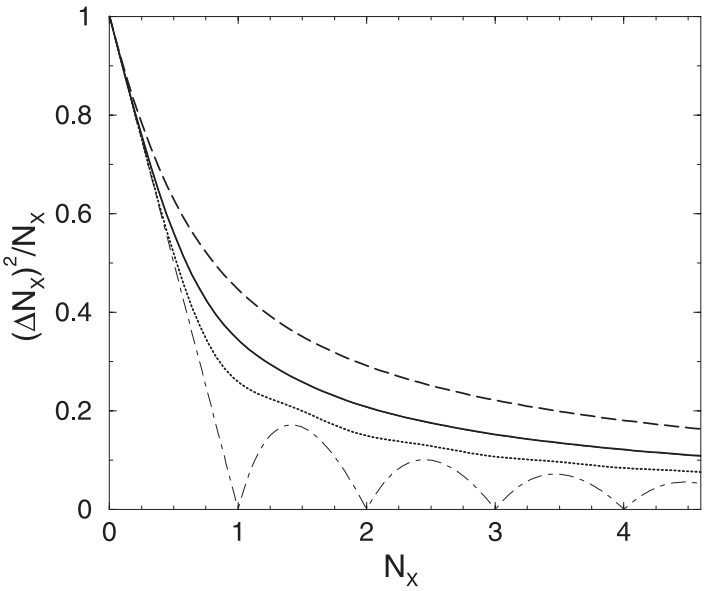

Figure 5. Particle-number fluctuation $(\Delta N_X)^2/N_X$ in domains X of the CS model after equation (5.2) for $\nu = 0$ (broken), $\frac{1}{2}$ (full) and $\frac{3}{2}$ (dotted). The chain curve corresponds to $(\Delta N_X)^2/N_X$ for strict correlation [3].

by [1, 3, 13]

$$\frac{(\Delta N_X)^2}{N_X} = 1 - \frac{1}{nX}\int_0^X \mathrm{d}x_1 \int_0^X \mathrm{d}x_2\, w(x_{12}) = 1 - \frac{1}{Y}\int_0^Y \mathrm{d}y_1 \int_0^Y \mathrm{d}y_2\, \frac{h(y_{12})}{\pi} \tag{5.1}$$

with $Y = k_F X = \pi n X$. Following appendix A of [3] the 2D integral (5.1) is reduced to a 1D integral with the help of the Fourier transform (4.13), namely

$$\frac{(\Delta N_X)^2}{N_X} = 1 - \frac{2}{Y}\int_0^\infty \frac{\mathrm{d}q}{\pi}\,\frac{1-\cos(qY)}{q^2}\,\frac{\tilde{h}(q)}{\pi}. \tag{5.2}$$

The results are shown in figure 5, where the case $\nu \to \infty$ ('strict' or 'perfect' correlation) [3] is also displayed. Traces of the oscillations as $\nu \to \infty$ are already visible for $\nu = \frac{3}{2}$.

With $h(y) = 1 - g(y)$ and with the expansion of $g(y)$ according to equation (4.1)—see also the text after equation (4.13)—the small-X expansion of equation (5.1) is

$$\frac{(\Delta N_X)^2}{N_X} = 1 + d_1 nX + d_2(nX)^2 + d_3(nX)^3 + d_4(nX)^4 + d_5(nX)^5 + \cdots. \tag{5.3}$$

The slope d_1 at $X = 0$ does not depend on the interaction strength parameter ν as shown in table 4 because of $g(0) = 0$ and $h(0) = 1$ not depending on ν; but the coefficients of the next terms do such that the particle-number fluctuations are suppressed due to repulsive particle interaction, but enhanced due to attractive particle interaction: correlation makes the particle-number distribution $P_X(N)$ narrower for repulsion ($\nu > \frac{1}{2}$) and broader for attraction ($\nu < \frac{1}{2}$). We remark, that fluctuation enhancement (induced by attractive interaction) may generally support/cause clusterings (e.g. paramagnons prior to the para-to-ferromagnetic phase

Table 4. Coefficients of the small-X expansion of $(\Delta N_X)^2/N_X$ as in equation (5.3).

ν	0	$\frac{1}{2}$	$\frac{3}{2}$
d_1	-1	-1	-1
d_2	$\frac{1}{18}\pi^2$	0	0
d_3	0	$\frac{1}{18}\pi^2$	0
d_4	$-\frac{1}{600}\pi^4$	0	0
d_5	0	$-\frac{2}{675}\pi^4$	$\frac{16}{2025}\pi^4$

transition). In our case this tendency shows up in the sudden 'fall-into-the-origin' at $\nu = 0$. If one considers with $X = 1/n$ a Wigner–Seitz 'sphere' (with 'radius' $X/2$ and $N_X = 1$), then

$$\Sigma_1(\nu) = 1 - \frac{\chi(\nu)}{\chi(\frac{1}{2})} \qquad \chi(\nu) = \frac{(\Delta N_X)^2}{N_X} \tag{5.4}$$

is a reasonable correlation measure based on particle-number fluctuations as we show in figure 6.

On-top behaviour. The exponent α and the coefficients A, a_i of equation (4.1) describe the short-range or dynamical correlation, i.e. the small-separation behaviour of $g(y)$, see table 1. Cioslowski's correlation cage [8] is in our case simply the inter-particle-separation range $y = 0 \ldots y_{\max}$ with $y_{\max}$ being that separation where the PD $g(y)$ has its first maximum $g_{\max} = g(y_{\max})$. For $\nu = 0, \frac{1}{2}, \frac{3}{2}$ the corresponding values are $y_{\max} = \infty, \pi$, 2.99 and $g_{\max} = 1, 1, 1.24$ [3]. One may ask to what extent the correlation cage contributes to the interaction energy and define

$$\Sigma_2(\nu) = 1 - \frac{V_{\text{cage}}(\nu)}{V_{\text{cage}}(\frac{1}{2})} \qquad V_{\text{cage}}(\nu) = \frac{\int_0^{y_{\max}} \mathrm{d}y\, g(y)/y^2}{\int_0^{\infty} \mathrm{d}y\, g(y)/y^2} \leqslant 1 \tag{5.5}$$

as an energetic correlation measure with $V_{\text{cage}}(0) = 1$; the expression simplifies when using (4.2). Both Σ_1 and Σ_2 vanish for $\nu = \frac{1}{2}$ as shown in figure 6.

5.2. Quantities following from the momentum distribution

Critical exponent. The critical or correlation exponent β of equation (4.4) can be computed from conformal field theory [15, 37]. It describes (together with the coefficient B) the behaviour of n_κ near $\kappa = 1$ according to equations (4.3*a*) and (4.3*b*). For the three special values $\nu = 0, \frac{1}{2}$ and $\frac{3}{2}$, this gives $\frac{1}{4}$, 0 and $\frac{1}{4}$, respectively, as shown in figure 6. The exponent γ describes the decay of the correlation tail.

Non-idempotency and correlation entropy. The qth-order non-idempotency is [12] $c(q) = 1 - \int_0^\infty \mathrm{d}\kappa\, (n_\kappa)^q$. The derivative of $c(q)$ at $q = 1$ is $s \equiv c'(1)$ or

$$s(\nu) = -\int_0^\infty \mathrm{d}\kappa\, n_\kappa \ln n_\kappa \geqslant 0 \tag{5.6}$$

to be referred to as correlation entropy [12, 13]. It has been plotted in figure 6.

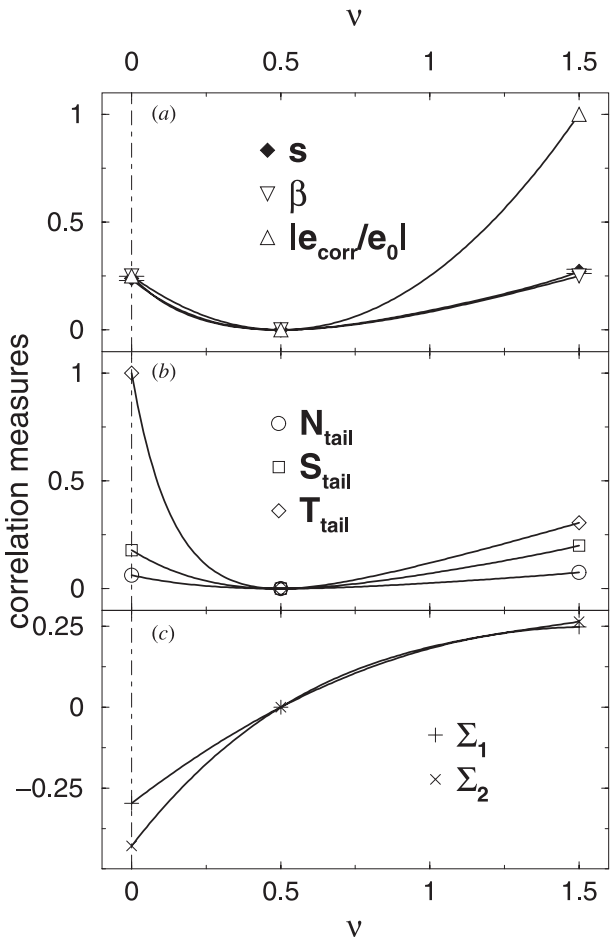

Figure 6. Correlation measures based on (*a*) the bulk of the momentum distribution, (*b*) the tail of the momentum distribution and (*c*) the PD shown as functions of ν. The full curves are guides to the eye only. The thin chain line indicates the 'fall-into-the-origin' at $\nu = 0$.

Correlation tail properties. The relative number of particles (or holes) in the corresponding correlation tail is [12, 13, 39]

$$N_{\rm tail}(\nu) = \int_1^\infty {\rm d}\kappa\, n_\kappa = \int_0^1 {\rm d}\kappa (1 - n_\kappa) < 1. \tag{5.7}$$

The contribution of the correlation tail to s is [13]

$$S_{\rm tail}(\nu) = -\int_1^\infty {\rm d}\kappa\, n_\kappa \ln n_\kappa < s(\nu). \tag{5.8}$$

In addition to these quantum-kinematic measures one may use [13]

$$T_{\rm tail}(\nu) = \frac{\int_1^\infty {\rm d}\kappa\, n_\kappa \kappa^2}{\int_0^\infty {\rm d}\kappa\, n_\kappa \kappa^2} \leqslant 1 \tag{5.9}$$

as another energetic measure with $T_{\rm tail}(0) = 1$. Also these correlation measures vanish for $\nu = \frac{1}{2}$ as shown in figure 6.

5.3. The correlation energy

For $e_{\rm corr} = e - e_{\rm HF}$ it follows that

$$e_{\rm corr} = -\left(\nu - \tfrac{1}{2}\right)^2 e_0. \tag{5.10}$$

The kinetic and interaction energy contribute $t_{\rm corr} = -\frac{1}{2\nu} e_{\rm corr}$ and $v_{\rm corr} = \left(1 + \frac{1}{2\nu}\right) e_{\rm corr}$, respectively, to $e_{\rm corr}$.

5.4. Comparison of the correlation measures

When comparing the computed correlation measures in figures 6 it turns out that for small $|\nu - \frac{1}{2}|$ the PD-based measures $\Sigma_{1,2}$ of equations (5.4) and (5.5) are proportional to $\nu - \frac{1}{2}$ (which is $-e'_{\rm corr}/(2e_0)$), whereas the n_κ-based measures (5.6)–(5.9) as well as (4.4) behave like $(\nu - \frac{1}{2})^2$ (which is $-e_{\rm corr}/e_0$). So the latter ones are not so sensitive as the first ones. With $s(\nu) = 0.5828|e_{\rm corr}/e_0| + \cdots$ the Collins' conjecture $|e_{\rm corr}| \sim s$ is confirmed at least for weak interaction. In this limit also $N_{\rm tail}$, $S_{\rm tail}$ and $T_{\rm tail}$ are mutually proportional and their derivatives are proportional to Σ_1 and Σ_2.

We note that the quantities $\chi(\nu)$, $V_{\rm cage}(\nu)$, $N_{\rm tail}(\nu)$, $S_{\rm tail}(\nu)$ and $T_{\rm tail}(\nu)$ are reference free, i.e. they are defined without reference to the non-interacting case $\nu = \frac{1}{2}$, which in our case is simultaneously equivalent to the Hartree–Fock approximation. Reference quantities appear in $\Sigma_{1,2}$ with $\chi(\frac{1}{2})$ and $V_{\rm cage}(\frac{1}{2})$ and in $s(\nu)$ with $s(\frac{1}{2}) = 0$. Whereas this observation is important for quantum chemistry—as stressed by J Cioslowski [8]—whenever multi-configuration appears, it is less important in our case which is well described by single configuration.

6. Numerical determination of 1PDM and $n(\kappa)$ for the CS model

Results from the theory of random matrices enable the calculation of various correlation functions for the CS model [14, 15, 28–30]. In particular, the 1PDM can be expressed in terms of a determinant of an appropriate matrix $F^{(\nu)}_{pq}$ [14, 15]. The size of this matrix is specified by the number of particles N to be $(N-1)^2$ for $\nu = \frac{1}{2}$ and $\frac{3}{2}$ and $(N-1)^2/4$ for $\nu = 0$. Each element of $F^{(\nu)}_{pq}$ contains simple trigonometric 1D ($\nu = \frac{1}{2}$ and $\frac{3}{2}$) or 2D ($\nu = 0$) integrals.

For some cases, most notably $\nu = \frac{1}{2}$, the resulting determinant can be computed analytically and corresponding expressions have been given in [15]. For the other cases, we have evaluated the determinant numerically [15], using a subdivision of the system volume (periodicity length) according to $L/L_0 = 42, 402$ and 402 for $\nu = 0$, $\frac{1}{2}$ and $\frac{3}{2}$, respectively. The particle number, odd due to periodicity of the wavefunction [15], varied from $N = 1$ to 401, corresponding to a variation in density n from nearly 0 to nearly 1. Taking the Fourier transform, we next compute the momentum distribution n_κ for all densities. In the inset of figure 3, we show results for one of the three special ν values.

Next, we apply the definitions of correlation measures and correlation energies as given in sections 3–5 and study their density dependence. In figure 7 we show results for the entropy s and in figure 8 for the various energies as the density is varied. As *all* energies scale with n^2, these measures should be *density independent* when normalized with respect to e_0. However, we do, in fact, see a pronounced density dependence for $n \gtrsim 0.5/L_0$ and also for $n \lesssim 0.05/L_0$. This latter density dependence is simply due to the small particle numbers, thus a small size of $F^{(\nu)}_{pq}$ and consequently a limited resolution when computing the 1PDM

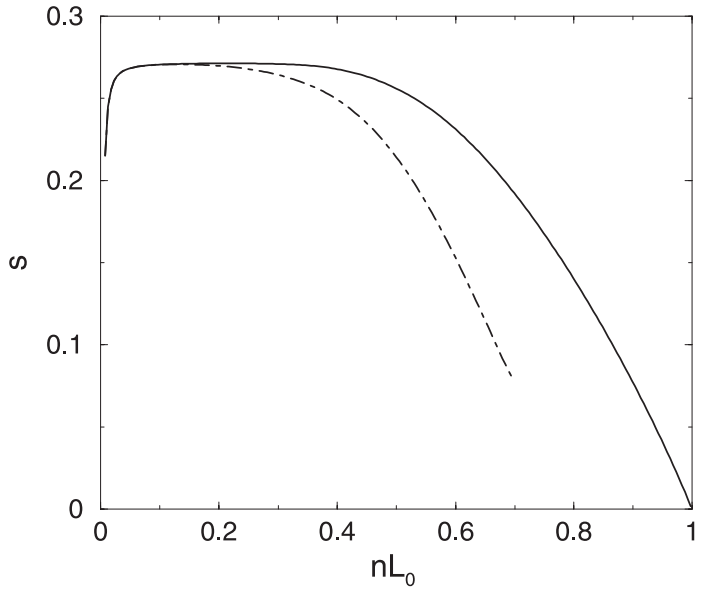

Figure 7. Correlation entropy (5.6) for fermions (full curve) as a function of density at $\nu = \frac{3}{2}$. The chain curve corresponds to s obtained for the discrete CS model.

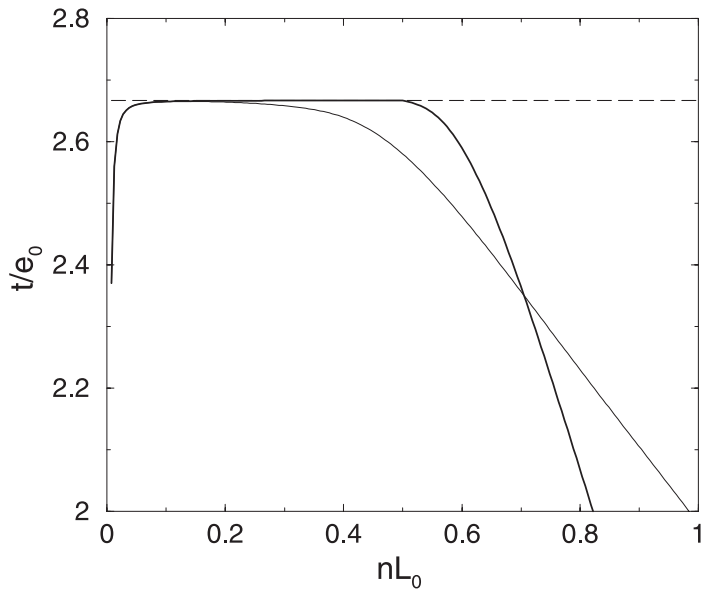

Figure 8. Kinetic energy t as computed from the Hellman–Feynman theorem (2.5) (broken line), and t from equation (2.6) (full curves) for fermions (thick curve) and bosons (thin curve) as a function of density at $\nu = \frac{3}{2}$.

at fixed L/L_0. The density dependence at large n values is more complicated to explain. The computation of the 1PDM by the connection with random matrix theory works for the

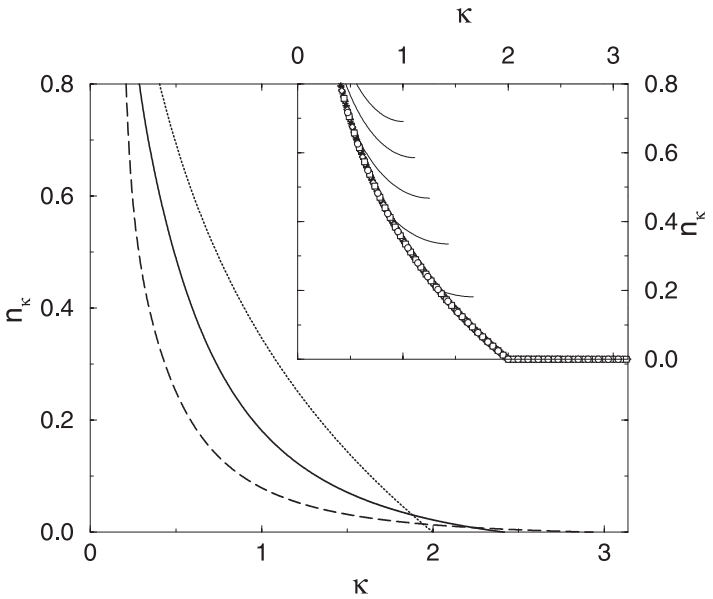

Figure 9. Bosonic momentum distributions n_κ versus $\kappa = k/k_F$ with $\nu = 0$ (broken), $\frac{1}{2}$ (full) and $\frac{3}{2}$ (dotted). Inset, n_κ for $\nu = \frac{3}{2}$, $L = 401$ and particle numbers identical to the inset of figure 3. The data for $N = 21(\circ)$, $41(\square)$, $81(\diamond)$, $121(\times)$, $161(+)$ and $201(*)$ do not show any density dependence effects.

periodic model[7]. Thus there exists a Brillouin zone and the tail of n_κ for $|\kappa|$ outside this Brillouin zone is folded back into it. The tail of n_κ thus tends to be dominated by this effect for large n values as shown in the inset of figure 3. However, knowing that the correlation measures must be independent of density in the thermodynamic limit, we deduce their values by restricting to these density regions where the independence holds. Then we apply the fit according to equation (4.3) as explained in section 4.2. In figure 6 we indicate by error bars the small variation in the correlation entropy when using instead of n_κ as in figure 3 the n_κ as in the inset. Similarly, the corresponding variations in N_{tail}, S_{tail} and T_{tail} are within the symbol sizes.

7. Extension to impenetrable bosons and lattice gases

As mentioned in the introduction, the CS model is also solvable for bosonic particle symmetry. The bosonic wavefunctions have to obey an additional boundary condition, namely they have to vanish for inter-particle separations $x_{ij} \to 0$ such that the resulting system consists of *impenetrable* or hard-core particles [14] with additional μ/x_{ij}^2 interaction. Both PD and 1PDM may be calculated as before. The PD is independent of statistics [14], thus the fermionic exchange hole agrees with the bosonic impenetrability hole and all quantities computed before based on the PD are the same in the bosonic and the fermionic case. For the 1PDM this is different, the momentum distribution of bosons is quite different from the fermionic n_κ as shown in figure 9. However, energetic quantities and correlation measures based upon those are nevertheless independent of the statistics and should thus be the same for bosons and fermions. In figure 8 we show that this is indeed the case. Thus, besides the density independence we

[7] See footnote 6.

have another criteria that allows us to extract the correct values of the correlation measures from these plots. We note that the above-mentioned unwanted density dependence is also present in the bosonic n_κ and visible in figures 7 and 8. Also present is the aliasing effect as shown in the inset of figure 9.

In [14, 15], it had been shown to be useful to restrict the family of wavefunctions of the CS model for both bosonic and fermionic symmetry to a lattice such that the coordinates are integers $x_j = 1, 2, \ldots L$ [40–42]. Only the normalization constants of the wavefunctions change and the 1PDM can be computed much as before [14], replacing the integrals in $F^{(\nu)}_{pq}$ by appropriate sums [15]. Furthermore, the structure factor $S(q)$ is known exactly and therefore so is the PD [15]. The resulting lattice gas has a particle–hole symmetry and thus we need to consider $n \leqslant \frac{1}{2}L_0$ only. However, the density N/L now enters all expressions in a non-trivial way and the very useful density independence of the continuum model for the quantities considered here is no longer applicable. Nevertheless, the continuum model corresponds to the low-density limit of the discrete model. In figure 7, we show that this is indeed the case for, for example, the correlation entropy.

8. Discussion and conclusions

Both the PD- and n_κ-based correlation measures (4.4) and (5.4)–(5.9) vanish for $\nu = \frac{1}{2}$ (no interaction). However, the first ones are more sensitive because of $\Sigma_{1,2} \sim \nu - \frac{1}{2}$ near to the no-interaction point as shown in figure 6(*c*), while the second ones are $\sim (\nu - \frac{1}{2})^2$ like $e_{\rm corr}$ of equation 5.10 as shown in figures 6(*a*) and (*b*) and therefore cannot distinguish between attractive and repulsive interactions. In 1D the PD-based measures (5.4) and (5.5) are identical for fermionic and (hard-core) bosonic particles. The n_κ-based measures (4.4) and (5.6)–(5.9) do not apply for bosonic particles; they are designed for fermionic particles only and appropriate bosonic variants still have to be defined.

For repulsive particle interaction results well known from other extended many-body systems, such as enhancement of the Friedel oscillations with maxima/minima trajectories (figure 2), humps/peaks of the static structure factor developing from its non-interacting kink (figure 4), suppression of particle-number fluctuations (figure 5), are confirmed again. However, for attractive interactions, we have found in this paper that particle-number fluctuations are *contrarily enhanced* and that this is accompanied by a smoothening of the PD (the oscillations disappear) and of the static structure factor (the kink disappears) as well as by the appearance of a linear on-top behaviour of the PD. The latter behaviour results in a diverging interaction energy in the strong attraction limit although the total energy remains finite. In momentum space the Fermi ice block thaws for both cases and correlation tails develop. In the strong attraction limit the correlation tail becomes so long ranged that the kinetic energy diverges, thereby exactly compensating the divergence of the interaction energy. We have shown that these divergences can be derived from the exactly known energy as a function of the interaction strength with the help of the Hellmann–Feynman theorem (2.5). This theorem allows one to calculate $t(\nu)$ and $v(\nu)$ separately from $e(\nu)$ and gives—in addition to their normalizations (3.2) and (3.4)—exact relations for n_κ and the PD as shown in equations (3.3) and (3.5) together with equations (4.7) and (4.8), respectively. Equations (3.6) and (4.9) give additional exact integral relations between n_κ and the PD. We expect that similar relations can be derived for correlation function results [43, 44] based on the theory of Jack symmetric polynomials for values $\nu = p/q$ with p and q relatively prime positive integers [34]. Thus an extension of our work to these ν is possible, albeit necessating a different approach for the numerically stable evaluation of the products of integrals.

In summary, we have analysed particle-number fluctuations and studied measures for the correlation strength based on the pair density and on the momentum distribution of the 1D quantum system of $1/x_{ij}^2$ interacting particles. We made extensive use of the available exact solution and applied the Hellmann–Feynman theorem to the CS model. Our results show that further work is called for in order to make the qualitative terms 'weak and strong correlation' quantitatively precise presumably with a variety of quantities instead of a single index [13].

Acknowledgments

RAR gratefully acknowledges support by the Deutsche Forschungsgemeinschaft (SFB393) and the hospitality of the Max-Planck-Institut für Physik komplexer Systeme (Dresden) for an extended stay where much of this work was started. PZ thanks the Max-Planck-Institut für Physik komplexer Systeme and P Fulde for supporting this work.

Appendix A. Certain integrals

The following identities are valid with $\mathrm{Si}(x) = \int_0^x \mathrm{d}y\,[\sin(y)/y]$:

$$\int_0^\infty \frac{\mathrm{d}x}{\pi}\frac{\sin x}{x} = \frac{\mathrm{Si}(\infty)}{\pi} = \frac{1}{2} \tag{A.1}$$

$$\int_0^\infty \frac{\mathrm{d}x}{\pi}\left(\frac{\sin x}{x}\right)^2 = \frac{1}{2} \tag{A.2}$$

$$\int_0^\infty \frac{\mathrm{d}x}{\pi}\,[\mathrm{Si}(\infty) - \mathrm{Si}(x)]\,\frac{\mathrm{d}}{\mathrm{d}x}\frac{\sin x}{x} = 0 \tag{A.3}$$

$$\int_0^\infty \frac{\mathrm{d}x}{\pi}\mathrm{Si}(x)\frac{\mathrm{d}}{\mathrm{d}x}\frac{\sin x}{x} = -\frac{1}{2} \tag{A.4}$$

$$\int_0^\infty \frac{\mathrm{d}x}{\pi}\frac{1}{x^2}\left[1 - \left(\frac{\sin x}{x}\right)^2\right] = \frac{1}{3} \tag{A.5}$$

$$\int_0^\infty \frac{\mathrm{d}x}{\pi}\frac{1}{x^2}\mathrm{Si}(x)\frac{\mathrm{d}}{\mathrm{d}x}\frac{\sin x}{x} = -\frac{2}{9}. \tag{A.6}$$

Equations (A.2)–(A.4) determine the normalization of the PDs (4.10)–(4.12). Equations (A.5) and (A.6) determine the interaction energy v for the HF approximation and for $\nu = \frac{3}{2}$. For the fluctuation analysis with equations (5.1) and (5.2)

$$\frac{2}{\pi}\int_0^\infty \mathrm{d}y\cos(qy)\left(\frac{\sin y}{y}\right)^2 = \left(1 - \frac{q}{2}\right)\theta(2-q) \tag{A.7}$$

$$\frac{2}{\pi}\int_0^\infty \mathrm{d}y\sin(qy)\,\mathrm{Si}(y)\frac{\sin y}{y} = -\frac{1}{2}\ln|1-q|\,\theta(2-q) \tag{A.8}$$

$$\frac{2}{\pi}\int_0^\infty \mathrm{d}y\cos(qy)\,\mathrm{Si}(y)\frac{\mathrm{d}}{\mathrm{d}y}\frac{\sin y}{y} = -\left[1 - \frac{q}{2} + \frac{q}{2}\ln|1-q|\right]\theta(2-q) \tag{A.9}$$

$$\int_0^\infty \mathrm{d}y\cos(qy)\frac{\mathrm{d}}{\mathrm{d}y}\frac{\sin y}{y} = -\left[1 - \frac{q}{2}\ln\left|\frac{1+q}{1-q}\right|\right] \tag{A.10}$$

$$\frac{2}{\pi}\int_0^\infty \mathrm{d}y\cos(qy)\frac{\sin y}{y}\frac{\mathrm{d}^2}{\mathrm{d}y^2}\frac{\sin y}{y} = \frac{1}{6}(q-2)\left(q^2 - q + 1\right)\theta(2-q) \tag{A.11}$$

$$2\pi \int_0^Y \mathrm{d}y_1 \int_0^Y \mathrm{d}y_2 \left(\frac{\sin|y_1 - y_2|}{|y_1 - y_2|} \right)^2 = 2 \int_0^2 \mathrm{d}q \, \frac{1 - \cos qY}{q^2} (1 - \tfrac{1}{2}q)$$
$$= 1 - \cos 2Y - 2Y\mathrm{Si}(2Y) + \int_0^{2Y} \mathrm{d}z \, \frac{1 - \cos z}{z}. \tag{A.12}$$

Appendix B. Kimball-like theorems for $n(x_{12})$ and n_κ

The small separation or on-top behaviour of the PD $n(x_{12})$ is derived here similarly to Kato [46] and Kimball [47] (see also [39, 45]) who found the cusp relation $\mathrm{d}g(k_\mathrm{F}r)/\mathrm{d}r|_{r=0} = g(0)/a_\mathrm{B}$ (or $g'(0) = \alpha r_s g(0), \alpha = (4/9\pi)^{1/3}$) for the pair correlation of the 3D uniform electron gas. Let us consider two adjacent electrons with the centre of mass and relative coordinates, $X = (x_1 + x_2)/2$ and $x = x_1 - x_2$, respectively. Focusing on the x dependence the Schrödinger equation can be written as

$$\left[-\frac{\mathrm{d}^2}{\mathrm{d}x^2} + \frac{\lambda(\lambda - 1)}{x^2} \right] \varphi(x)\tilde{\Phi}(X, x_3, \ldots) = (E - H')\varphi(x)\tilde{\Phi}(X, x_3, \ldots) \tag{B.1}$$

where H' contains the remaining terms in the Hamiltonian. Because $E - H'$ is non-singular as x approaches zero, it is unimportant for small x. To lowest order in x we therefore have $\varphi(x) = x^\lambda + \cdots$, from which immediately follows $n(x) \sim x^{2\lambda}$ for the PD, see equation (4.1). This can be concluded for $\lambda \neq 1$ also directly from the many-body wavefunction $\Phi \sim \prod_{i<j} x_{ij}^\lambda$ [14] and for $\lambda = 1$ from equation (4.11).

A similar treatment of the asymptotic large-κ behaviour of the momentum distribution n_κ seems to lead in equation (4.3c) to the conclusion $\gamma = 2\lambda + 2$. This corresponds to $n_{\kappa\to\infty} \sim g(0)/\kappa^8$ for the 3D uniform electron gas [39, 45, 47].

References

[1] Fulde P 1995 *Electron Correlations in Molecules and Solids* (Berlin: Springer)
[2] Schautz F, Flad H-J and Dolg M 1998 *Theor. Chem. Acc.* **99** 231 and references cited therein
[3] Ziesche P, Tao J, Seidl M and Perdew J P 2000 *Int. J. Quantum Chem.* **77** 819
[4] Kurth S and Perdew J P 2000 *Int. J. Quantum Chem.* **77** 814
[5] Bader R F W 1990 *Atoms in Molecules* (Oxford: Clarendon)
[6] Aslangul C, Constanciel R, Daudel R and Kottis Ph 1972 *Adv. Quantum Chem.* **6** 93 and references cited therein
[7] Dobson J F 1991 *J. Chem. Phys.* **94** 4328
[8] Cioslowski J and Liu G 1999 *J. Chem. Phys.* **110** 1882 and references cited therein
[9] Löwdin P-O 1955 *Phys. Rev.* **97** 1474
[10] Collins D M 1993 *Z. Natur.* **48a** 68
Collins D M 1992 *Acta Crystallogr.* A **49** 86
[11] Ramirez C J, Pérez J H M, Sagar R P, Esquivel R O, Hô M and Smith V H Jr 1998 *Phys. Rev.* A **58** 3507 and references cited therein
[12] Ziesche P, Gunnarsson O, John W and Beck H 1997 *Phys. Rev.* B **55** 10 270
Ziesche P, Smith V H Jr, Hô M, Rudin S P, Gersdorf P and Taut M 1999 *J. Chem. Phys.* **110** 6135 and references cited therein
[13] Ziesche P 2000 *J. Mol. Struct.* **527** 35
[14] Sutherland B 1971 *J. Math. Phys.* **12** 246
Sutherland B 1971 *J. Math. Phys.* **12** 251
Sutherland B 1971 *Phys. Rev.* A **4** 2019
Sutherland B 1972 *Phys. Rev.* A **5** 1372
[15] Sutherland B 1992 *Phys. Rev.* B **45** 907
Römer R A and Sutherland B 1993 *Phys. Rev.* B **48** 6058
[16] Mehta M L 1990 *Random Matrices* (Boston, MA: Academic)
[17] Dyson F 1962 *J. Math. Phys.* **3** 140

[18] Szabo A and Ostlund N S 1982 *Modern Quantum Chemistry* (New York: McGraw-Hill)
[19] Hammond B L, Lester W A Jr and Reynolds P J 1994 *Monte Carlo Methods in Ab Initio Quantum Chemistry* (Singapore: World Scientific)
[20] Mazziotti D A 1999 *Phys. Rev.* A **60** 4396
Ehara M 1999 *Chem. Phys. Lett.* **305** 483
Valdemoro C, Tel L M and Pérez-Romero E 2000 *Phys. Rev.* A **61** 032507
[21] Fulde P, Stoll H and Kladko K 1999 *Chem. Phys. Lett.* **299** 481
[22] Polyakov A M 1970 *Pis. Zh. Eksp. Teor. Fiz.* **12** 538 (Engl. transl. 1970 *JETP Lett.* **12** 381)
[23] Belavin A A, Polyakov A M and Zamolodchikov A B 1984 *Nucl. Phys.* B **241** 333
[24] Cardy J L 1984 *Phys. Rev. Lett.* **52** 1575
[25] Cardy J L 1987 *Phase Transitions and Critical Phenomena* vol 11, ed C Domb and J L Lebowitz (New York: Academic)
[26] Sutherland B and Römer R A 1993 *Phys. Rev. Lett.* **71** 2789
[27] Sutherland B, Römer R A and Shastry B S 1994 *Phys. Rev. Lett.* **73** 2154
[28] Simons B D and Altshuler B L 1993 *Phys. Rev. Lett.* **70** 4063
[29] Simons B D and Altshuler B L 1993 *Phys. Rev.* B **48** 5422
[30] Kravtsov V E and Tsvelik A M 2000 *Phys. Rev.* B **62** 9888
(Kravtsov V E and Tsvelik A M 2000 *Preprint* cond-mat/0002120)
[31] Olshanetsky M A and Perelomov A M 1981 *Phys. Rep.* **71** 313
[32] Hellmann H 1937 *Einführung in die Quantenchemie* (Leipzig: Deuticke) pp 61, 285 (the original Russian version is Gel'man G 1936 *Quantenchemie* (Moscow and Leningrad: ONTI) p 428)
Feynman R P 1939 *Phys. Rev.* **56** 340
[33] Landau L D and Lifshitz E M 1977 *Quantum Mechanics* (Oxford: Pergamon) section 35
[34] Ha Z N C 1996 *Quantum Many-Body Systems in One Dimension* (Singapore: World Scientific)
[35] Haldane F D M 1981 *J. Phys. C: Solid State Phys.* **14** 2585
[36] Schulz H J, Cuniberti G and Pieri P 2000 *Field Theories in Low-Dimensional Condensed Matter Systems* ed G Morandi *et al* (Berlin: Springer)
(Schulz H J, Cuniberti G and Pieri P 1998 *Preprint* cond-mat/9807366)
[37] Kawakami N and Yang S-K 1991 *Phys. Rev. Lett.* **67** 2493
[38] Yokoyama H and Ogata M 1991 *Phys. Rev. Lett.* **67** 3610
[39] Takada Y and Yasuhara H 1991 *Phys. Rev.* B **44** 7879
[40] Gebhardt F and Vollhardt D 1987 *Phys. Rev. Lett.* **59** 1472
[41] Shastry B S 1988 *Phys. Rev. Lett.* **60** 639
[42] Haldane F D M 1988 *Phys. Rev. Lett.* **60** 635
[43] Ha Z N C 1994 *Phys. Rev. Lett.* **73** 1574
Lesage F, Pasquier V and Serban D 1995 *Nucl. Phys.* B **435** 585
[44] Forrester P J 1995 *Mod. Phys. Lett.* B **9** 359
[45] Yasuhara H and Kawazoe Y 1976 *Physica* A **85** 416
[46] Kato T 1957 *Commun. Pure Appl. Math.* **10** 151
see also Pack R T and Brown W B 1966 *J. Chem. Phys.* **45** 556
Chang S Y, Davidson E R and Vincow G 1970 *J. Chem. Phys.* **52** 1740
[47] Kimball J C 1975 *J. Phys. A: Math. Gen.* **8** 1513
[48] Güttinger P 1932 *Z. Phys.* **73** 169
[49] Born M and Fock V 1928 *Z. Phys.* **51** 165
[50] Schrödinger E 1926 *Ann. Phys., Lpz.* **80** 437